Simulating the effects of climate change on tropical montane cloud forests

Christopher J. Still*‡, Prudence N. Foster† & Stephen H. Schneider*

* *Department of Biological Sciences, Stanford University, Stanford, California 94305-5020, USA*
† *Center for Climate Studies Research, University of Tokyo, Komaba 4-6-1, Meguro-ku, Tokyo 153-8904, Japan*
‡ *Carnegie Institution of Washington, Department of Plant Biology, 260 Panama Street, Stanford, California 94305-4150, USA*

Tropical montane cloud forests are unique among terrestrial ecosystems in that they are strongly linked to regular cycles of cloud formation. We have explored changes in atmospheric parameters from global climate model simulations of the Last Glacial Maximum and for doubled atmospheric carbon dioxide concentration ($2 \times CO_2$) conditions which are associated with the height of this cloud formation, and hence the occurrence of intact cloud forests. These parameters include vertical profiles of absolute and relative humidity surfaces, as well as the warmth index[1], an empirical proxy of forest type. For the glacial simulations, the warmth index and absolute humidity suggest a downslope shift of cloud forests that agrees with the available palaeodata. For the $2 \times CO_2$ scenario, the relative humidity surface is shifted upwards by hundreds of metres during the winter dry season when these forests typically rely most on the moisture from cloud contact. At the same time, an increase in the warmth index implies increased evapo-transpiration. This combination of reduced cloud contact and increased evapo-transpiration could have serious conservation implications, given that these ecosystems typically harbour a high proportion of endemic species and are often situated on mountain tops or ridge lines.

Tropical montane cloud forests (TMCFs) occur where mountains are frequently enveloped by tradewind-derived orographic clouds and mist in combination with convective rainfall. Many features of these forests are directly or indirectly related to cloud formation, from vegetation morphology to nutrient budgets to solar insolation[2]. One of the most direct impacts of frequent cloud cover is the deposition of cloud droplets through contact with soil and vegetation surfaces (horizontal precipitation)[3]. Total horizontal precipitation is greater than that from vertical rainfall events in some systems during the dry season, when these forests can experience water stress[2,4]. Because the combination of horizontal precipitation and lowered evapo-transpiration due to frequent cloud contact significantly increases precipitation minus evaporation in these forests, they function as important local and regional watersheds. Also, owing to the sponge-like effect of epiphytes (for example, mosses, bromeliads and ferns), these forests act as capacitors in regulating the seasonal release of precipitation, thereby providing flood and erosion control in the rainy season and water storage in the dry season.

In addition to their hydrological importance, these ecosystems typically harbour an impressive array of plants and animals. Although the biodiversity of TMCFs is not as high as that of lowland moist tropical forests[5], the level of endemism found in resident animal species is exceptional[3]. For example, 32% of Peruvian endemic vertebrates are localized in cloud forests[6]. The conservation status of these unique ecosystems is precarious as they are among the most endangered of all tropical forest types. A high annual deforestation rate in tropical mountain forests caused by harvesting fuel wood, resource logging and agricultural conversion is increasingly threatening cloud forests worldwide[5].

Palaeoclimatic pollen evidence strongly suggests a downslope shift of the range of some current cloud forest species during the last glacial period. There is abundant evidence[7] for downslope migrations of South and Central American montane taxa (*Quercus*, *Alnus*, *Weinmannia* and *Podocarpus*, for example) during glacial times. *Weinmannia* is now a characteristic genus of cloud forest trees in the high Andes, and *Podocarpus* is found in cloud forests throughout the tropics. Other evidence, ranging from noble gas concentrations in groundwater[8] to Barbados corals[9], to snowline depression[10], indicates that certain regions of the tropics were cooler by some 2–5 °C, with considerable variation in both temperature and moisture conditions[11,12]. Such changes surely affected both the altitudinal and latitudinal distributions of cloud forests in the glacial past.

Cloud formation associated with trade winds often occurs as a result of orographic effects. For example, in Costa Rica the humid trade winds from the Caribbean Sea quickly encounter the continental divide formed by the Cordillera de Tilarán in the north-central portion of the country and the prevailing winds undergo orographic uplift[13]. As these air parcels are uplifted, they expand and cool until their water vapour pressure exceeds their saturation vapour pressure and condensation can occur. The clouds formed in this process are referred to as orographic clouds, and the height at which water vapour condenses is the lifting condensation level (LCL).

This altitude is a function of the lapse rate, which decreases from a dry adiabatic rate to a moist adiabatic rate when condensation occurs during rapid ascent of an air parcel. A moist adiabatic ascent causes a given increase in surface temperature to be amplified with height. An early-generation general circulation model (GCM) that parameterized subgrid-scale convection by using dry and moist convection lapse rate adjustments, showed that an imposed 2 °C warming (cooling) of sea surface temperatures (SSTs) caused a +2.4 °C (−2.78 °C) response of simulated atmospheric temperatures at 1.5 km, and a +3.52 °C (−3.45 °C) response at 4.5 km (ref. 14). Such an amplification of surface warming with height was also found over the tropics in a classical $4 \times CO_2$ GCM experiment[15] and was observed in the real atmosphere over the tropics[16]. A shift to a more moist adiabatic lapse rate in low latitudes as a result of an enhanced hydrological cycle has been suggested, which could influence the height of the freezing level surface[17] or the height at which orographic clouds form.

The rapid melting of high mountain glaciers in low latitudes[18,19] has been related to the observed warming of tropical ocean surfaces[17], which in turn correlates with increases in tropospheric

Table 1 Simulated values of parameters (GENESIS GCM)

	Parameter	Monteverde	Serrenia	Mt Kinabalu	Mt Virunga
1	$\Delta T(2 \times CO_2)$	2.1	2.1	2.2	2.5
2	ΔT(LGM)	−2.4	−2.2	−2.1	−1.9
3	ΔAH($2 \times CO_2$)	16	13	17	15
4	ΔAH(LGM)	−11	−15	−15	−13
5	$\Delta W_I(2 \times CO_2)$	25.3	25.0	25.9	29.4
6	ΔW_I(LGM)	−28.6	−26.8	−25.5	−22.9
7	$\Delta Z_{RH}(2 \times CO_2)$ DJF	228	109*	176	98
8	$\Delta Z_{RH}(2 \times CO_2)$ JJA	−127	−34	−20	−156
9	ΔZ_{RH}(LGM) DJF	93	−40*	−454	−111
10	ΔZ_{RH}(LGM) JJA	−103	270	625	−43.8
11	$\Delta Z_{AH}(2 \times CO_2)$ DJF	301	295	332	341
12	$\Delta Z_{AH}(2 \times CO_2)$ JJA	276	227	285	183
13	ΔZ_{AH}(LGM) DJF	−162	–	−480	−242
14	ΔZ_{AH}(LGM) JJA	−290	−168	−236	−161
15	$\Delta Z_{W_I}(2 \times CO_2)$	442	329	492	442
16	ΔZ_{W_I}(LGM)	−424	−298	−439	−320
17	LCL (DJF)	657	1,082	543	1,521
18	LCL (JJA)	510	719	577	1,634

Rows 1–6 show the difference in the annual temperature (°C), absolute humidity (AH; %) and warmth index (W_I; °C-months) between the alternate climate experiments and the control run for each cloud forest location. The ΔZ rows (7–16) show the altitude shift (metres) required to reproduce the target proxy in the alternative climates (see text for details), averaged over summer (JJA) and winter (DJF) months, where appropriate. Rows 7–10 show the shift for RH; rows 11–14 for AH; and rows 15, 16 for W_I. A dash indicates that the proxy value was not reproduced in the alternative climate simulation for any of the 3 months in the season; an asterisk indicates that the proxy was reproduced in only one month. Rows 17, 18, seasonally averaged LCL.

© 1999 Macmillan Magazines Ltd

moisture content[16,20,21]. Specifically, analysis of decadal-scale trends of specific humidity, relative humidity, and temperature over the tropical western Pacific revealed that all have increased throughout the troposphere since the mid-1970s (ref. 16). GCMs driven by these observed increases in tropical SSTs reproduce the observed tropospheric warming from the 1970–1992 period primarily by hydrological cycle responses (that is, an increase in the global release of latent heat[20]). Moreover, an intensifying tropical hydrological cycle and associated changes in tropical circulation are suggested by analysis of COADS data[22]. However, although lower atmospheric specific humidity and temperature are very likely to increase in response to oceanic surface warming, cloud formation depends on relative humidity, and thus the influence of surface warming on the probability of cloud formation at current cloud forest altitudes is not straightforward.

A direct estimate for the altitude of cloud formation is the point at which supercooled water condenses onto cloud condensation nuclei, corresponding to a vapour relative humidity of over 100%. This microscale description cannot be applied explicitly in GCMs, because they have horizontal grid resolutions larger in size than any individual cloud and vertical resolutions of several hundreds of metres. Parametric representations of such sub-grid-scale phenomena, like clouds, have been tested[23], and show that GCMs do predict large-scale (that is, grid-box-scale) variables which are highly correlated with cloud formation and occurrence (for example, water vapour, lapse rate, temperature and vertical velocity). We have explored the use of two quantities that are determined by these variables: the grid-box-averaged relative humidity (RH) and the LCL.

The simulation results for the LCL are presented in Table 1. Neither the GENESIS model nor another GCM from the University of Illinois (data not shown) produces grid-scale LCLs in the control simulation that coincide with current cloud forest altitudes. Indeed, GCMs are not expected to produce highly accurate simulations of the absolute value of hydrological parameters like the amount of water vapour at individual grid boxes[23], particularly near the steep topography that characterizes cloud forest locations. Thus, we focus on the RH as a grid-scale cloud formation proxy, especially differences in the RH between simulations.

Relative humidity changes are not easily predictable as it is not obvious in advance whether specific humidity increases enough locally in the $2 \times CO_2$ experiment, for example, to overcome the increase in saturation vapour pressure locally. In some GCM experiments with imposed SST increases[14], RH decreased on average at an altitude of about 3 km (a typical cloud height) even though it increased near the surface. Similar results were obtained for a quadrupling of CO_2 (ref. 15). In Fig. 1b, our results show that the RH surface does not exhibit a consistent behaviour at the four cloud forest sites in the LGM simulation. However, the RH surface is consistently shifted upwards in the Northern Hemisphere winter season (December, January, February; DJF) at all of the sites in the $2 \times CO_2$ simulation. Opposite sign results for ΔZ_{RH} are obtained for the Northern Hemisphere summer season (June, July, August; JJA) at these same sites. We caution that the ΔZ_{RH} result should be viewed only as a crude proxy for cloud height change. Nevertheless, the RH surface of the Monteverde grid location (see Methods), for example, does suggest for the $2 \times CO_2$ case a rise of over 200 m in cloud height in winter, part of the dry season when that cloud forest relies most on the horizontal precipitation from cloud mists. Such a rise would imply a reduced frequency of contact and less horizontal precipitation, which would probably be of biological and hydrological significance to the cloud forest's structure and functioning.

As an alternative to predicting cloud heights to assess the impact of climate change on cloud forests, we relied upon the principles of biogeography models to predict the location of cloud forests in alternate climates. These models predict ecosystem locations using cutoffs in temperature sums and moisture balance calculations[24]. One temperature sum is the warmth index (W_I), which represents the sum of all monthly mean temperatures exceeding 5 °C (ref. 1). The upper limit of the cloud forest on Mt Kinabalu (see Methods) corresponds to a cutoff in the W_I of 85 °C-months[25], perhaps a result of the linear relationship between the W_I and potential evapotranspiration[26]. Actual evapo-transpiration varies linearly with net above-ground productivity[24], which can be successfully tied to ecosystem type[27]. Therefore, it is not surprising that the W_I is found to correlate broadly with forest type. In addition, we calculate the absolute humidity (AH) as a measure of the atmospheric water content at cloud forest elevations because moisture balance is also an important determinant of ecosystem type.

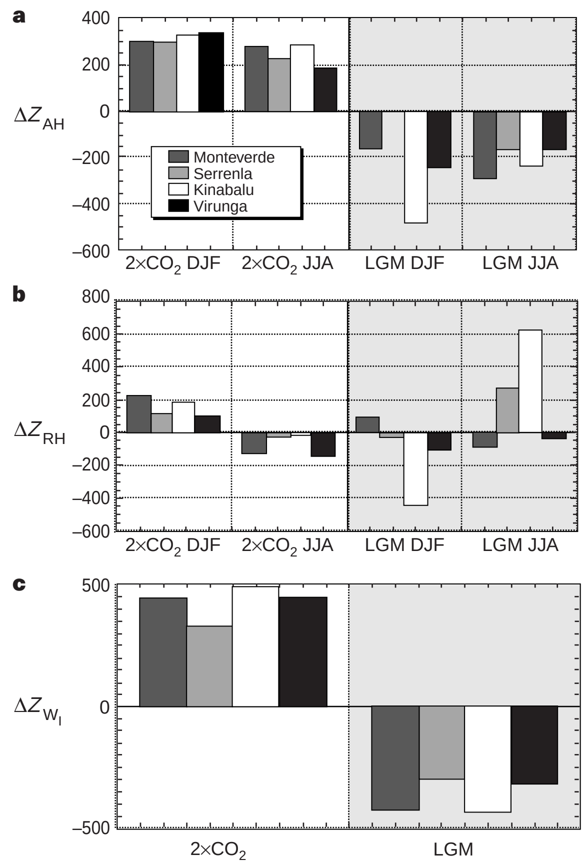

Figure 1 The shift in altitude, ΔZ, from the current cloud forest altitude that is required to reproduce a target climatic value (the variable's value at the cloud forest elevation in a GENESIS GCM control simulation) in a $2 \times CO_2$ or LGM simulation. The signal for summer (JJA) and winter (DJF) shifts are shown for **a**, the absolute humidity; and **b**, relative humidity; in **c**, only the yearly sum for the warmth index is shown. Left panels, ΔZ in the $2 \times CO_2$ simulation for four cloud forest locations; right panels, the LGM shift.

Figure 1a shows altitude shifts in the cloud forest absolute humidity surface in the GENESIS GCM for the $2 \times CO_2$ (ref. 28) and LGM[29] experiments: all four widely separated current cloud forest locations experience an increase in absolute humidity when global surface temperatures are warmer, as well as a decrease when it is cooler. This is anticipated, as warmer surface temperatures associated with $2 \times CO_2$ simulations cause increased evapo-transpiration and thus the altitude at which some absolute humidity surface would occur in the control experiment is expected to rise (it rises by ~300 m) in the $2 \times CO_2$ simulation; likewise, a descent (by ~200–500 m) in the LGM experiment is not unexpected.

Figure 1c shows the shift in altitude required to reproduce the W_I in alternate climates. As expected, the W_I decreases in the LGM experiment and increases in the $2 \times CO_2$ case. The predicted altitude shift in W_I is very similar to that of AH, suggesting that both the temperature and the moisture conditions of the current

© 1999 Macmillan Magazines Ltd

cloud forest will be reproduced at this shifted altitude. Because the warmth index and absolute humidity together reflect components of many contemporary biogeography models, the agreement in their altitude shifts is noteworthy. The results are suggestive because of the uniformity and comparable magnitude of many of our multiple proxy results, the agreement with ice-age pollen shifts, and our technique's reliance on simulation differences as opposed to absolute values (differences in GCM variables are often thought to be more reliable than absolute values).

The results of Pounds *et al.*[30], which track invasions of premontane species into cloud forest habitat near Monteverde, Costa Rica, provide further evidence of the climate sensitivity of these ecosystems. Notably, they have rejected habitat destruction pressures at lower elevations as a cause of this upslope movement. Thus, this and other cloud forests may be experiencing the dual stresses of changing microclimates and invading species from lower elevations, driven in part by changes in the height of orographic cloud bank formation in the dry season and/or increased evapo-transpiration. In light of these observations and our modelling results, the impact of climate change on cloud forests needs further investigation. In addition to using more sophisticated biogeography models and higher-resolution climate-change scenarios from additional GCMs, future work should involve GCMs driven by the observed trend in tropical SSTs[17,20] to examine present-day changes affecting these ecosystems. More realistic analyses at each of our TMCF sites will require transient GCM simulations combined with statistical downscaling techniques[23] and/or coupled mesoscale regional models that better resolve the steep topographic conditions and local land use changes at most cloud forest sites. Also, in addition to focusing on changes in the vertical distribution of cloud decks, changes in the latitudinal distribution of circulation systems and trade wind belts and the implications for cloud forests should be investigated. However, the implications of even our crude proxy results are clear: climate change will probably affect the distribution of the potential locations for cloud forests and, if our analysis proves credible, it may force those situated near mountain tops out of existence. □

Methods

We investigated the impact of climate change on four cloud forest locations, which span four continents, with a variety of altitudes and ocean proximities. The first site is the Monteverde cloud forest (84.8° W, 10.3° N, 1,500 m) in Costa Rica, which we chose owing to the breadth of climate, vegetation and zoological research ongoing there. As this location is an ocean cell in our GCM, we used the adjacent eastward land cell to examine a potential response at Monteverde. In South America, we chose the cloud forest at Serrania de Macuira (71.5° W, 12.5° N, 865 m), which sits on a peninsula on the northern shore of Colombia at a relatively low altitude. Mount Kinabalu (116.3° E, 6.5° N, 2,500 m), our third site, is located on the island of Borneo. Our final site, Mount Virunga (29.5° E, 1.8° S, 3,000 m) in Africa, is home to the severely endangered mountain gorilla. This high-altitude cloud forest is land-locked, although it is close to Lake Victoria.

We used the global climate model GENESIS version 2 (ref. 28) to predict changes in the elevation of cloud forests for three simulations: today (control), the LGM[29], and a CO_2-doubled atmosphere[28]. The simulations include a dynamic sea–ice model, a land–surface transfer scheme, a six-layer soil model and a 50-m slab mixed-layer ocean. The resolution of the simulations is spectral T31 ($\sim$3.75° longitude and latitude), with 18 vertical levels. The CO_2 concentration for the LGM was reduced by a specific percentage relative to the control that corresponds to the CO_2 lowering from the pre-industrial era to the LGM, insolation was set for the Earth orbit at 21 kyr, and ICE-4g ice sheets were prescribed. The $2 \times CO_2$ simulation was identical to the control run, except that the CO_2 concentration was doubled from 345 to 690 p.p.m.v. For each simulation, we used the monthly means, further averaged over ten years of each run, of the following variables: the pressure p, the specific humidity q, the air temperature T, and the elevation Z, of each grid level above mean sea level.

We determined the altitude shift of the relative humidity proxy, for example, as follows. We computed the simulated relative humidity surface, RH_{CF}, at the altitude of each of the TMCF sites, Z_{CF}, for today's climate (the control). We then compute, by linear interpolation (logarithmic interpolation produces similar results) between vertical levels in the GCM, the altitude, Z'_{CF}, at which RH_{CF} is reproduced at each TMCF grid box for both LGM and $2 \times CO_2$ climate change experiments. The difference, $\Delta Z_{RH} = Z'_{CF} - Z_{CF}$, is the predicted altitude shift. These results are shown in Table 1, together with calculations of the changes in temperature, absolute humidity and W_I. Note that we do not search for the altitude at which the RH surface reaches 100% in this technique, because in the real atmosphere cloudiness often persists at grid-box-averaged RH values of much less than 100%, when only part of a grid box is cloud-covered. The same technique is used for ΔZ_{AH} and ΔZ_{W_I}. Comparison of the W_I in climate change minus control simulations relies only on temperautre differences: thus, major systematic errors in absolute temperature should cancel out. To estimate the error in our altitude shift calculations requires knowledge of the accuracy of the $2 \times CO_2$ simulations, which is unknown. We performed a simple error analysis by arbitrarily assuming that each monthly temperature in the $2 \times CO_2$ simulation was too warm by 1 °C: then the altitude shift error for the W_I is 180 m, which is less than our calculated altitude shifts for this proxy.

Received 24 November 1998; accepted 25 February 1999.

1. Kira, T. *Terrestrial Ecosystems* (Kyoritsu, Tokyo, 1976).
2. Bruijnzeel, L. A. & Proctor, J. in *Tropical Montane Cloud Forests* (eds Hamilton, L. S., Juvik, J. O. & Scatena, F. N.) 38–78 (Springer, New York, 1995).
3. Stadtmüller, T. *Cloud Forests in the Humid Tropics: A Bibliographic Review* (The United Nations University, Tokyo, and Centro Agronomico Tropical de Investigacion y Ensenanza, Turrialba, Costa Rica, 1987).
4. Bruijnzeel, L. A. *Hydrology of Moist Tropical Forests and Effects of Conversion: A State of Knowledge Review* (IHP-UNESCO Humid Tropical Programme, Paris, 1990).
5. Hamilton, L. S., Juvik, J. O. & Scatena, F. N. in *Tropical Montane Cloud Forests* (eds Hamilton, L. S., Juvik, J. O. & Scatena, F. N.) 1–23 (Springer, New York, 1995).
6. Leo, M. in *Tropical Montane Cloud Forests* (eds Hamilton, L. S., Juvik, J. O. & Scatena, F. N.) 198–211 (Springer, New York, 1995).
7. Colinvaux, P. A., De Oliveira, P. E., Moreno, J. E., Miller, M. C. & Bush, M. B. A long pollen record from lowland Amazonia: forest and cooling in glacial times. *Science* **275,** 85–88 (1996).
8. Stute, M. *et al*. Cooling of tropical Brazil (5 °C) during the last glacial maximum. *Science* **269,** 379–383 (1995).
9. Guilderson, T. P., Fairbanks, R. G. & Rubenstone, J. L. Tropical temperature variations since 20,000 years ago: modulating interhemispheric climate-change. *Science* **263,** 663–665 (1994).
10. Rind, D. & Peteet, D. Terrestrial conditions at the last glacial maximum and CLIMAP sea-surface temperature estimates: Are they consistent? *Quat. Res.* **24,** 1–22 (1985).
11. Thompson, L. G. *et al*. Late glacial stage and Holocene tropical ice core records from Huascaran, Peru. *Science* **269,** 46–50 (1995).
12. Thompson, L. G. *et al.* A 25,000-year tropical climate history from Bolivian ice cores. *Science* **282,** 1858–1864 (1998).
13. Barros, A. P. & Lettenmaier, D. P. Dynamic modeling of orographically induced precipitation. *Rev. Geophys.* **32,** 265–284 (1994).
14. Schneider, S. H., Washington, W. M. & Chervin, R. M. Cloudiness as a climatic feedback mechanism: effects on cloud amounts of prescribed global and regional surface temperature changes n the NCAR-GCM. *J. Atmos. Sci.* **35,** 2207–2221 (1978).
15. Manabe, S. & Wetherald, R. T. On the distribution of climate change resulting from an increase in CO_2 content of the atmosphere. *J. Atm. Sci.* **37,** 99–118 (1980).
16. Gutzler, D. S. Climatic variability of temperature and humidity over the tropical western Pacific. *Geophys. Res. Lett.* **19,** 1595–1598 (1992).
17. Diaz, H. F. & Graham, N. E. Recent changes in tropical freezing heights and the role of sea surface temperature. *Nature* **383,** 152–155 (1996).
18. Hastenrath, S. & Kruss, P. The dramatic retreat of Mount Kenya's glaciers 1963–87: greenhouse forcing. *Ann. Glaciol.* **16,** 127–133 (1992).
19. Thompson, L. G. *et al.* Recent warming: ice core evidence from tropical ice cores with emphasis on central Asia. *Glob. Planet. Change* **7,** 145–156 (1993).
20. Graham, N. E. Simulation of recent global temperature trends. *Science* **267,** 666–671 (1995).
21. Gaffen, D. J., Barnett, T. P. & Elliott, W. P. Space and time scales of global tropospheric moisture. *J. Climate* **4,** 989–1008 (1991).
22. Flohn, H. & Kapala, A. Changes of tropical air–sea interaction processes over a 30-year period. *Nature* **338,** 244–246 (1989).
23. IPCC (Intergovernmental Panel on Climate Change) *Climate Change 1995: The Science of Climate Change* (eds Houghton, J. T. *et al.*) (Cambridge University Press, Cambridge, 1996).
24. Woodward, F. I. *Climate and Plant Distribution* (Cambridge University Press, Cambridge, 1987).
25. Kitayama, K. An altitudinal transect study of the vegetation on Mount Kinabalu, Borneo. *Vegetatio* **102,** 149–171 (1992).
26. Fang, J.-Y. & Yoda, K. Climate and vegetation on China II. Distribution of main vegetation types and thermal climate. *Ecol. Res.* **4,** 71–83 (1989).
27. Neilson, R. P. A model for predicting continental-scale vegetation distribution and water balance. *Ecol. Appl.* **5,** 362–385 (1992).
28. Thompson, S. L. & Pollard, D. Greenland and Antarctic mass balances for present and doubled CO_2 from the GENESIS version-2 global climate model. *J. Climate* **10,** 871–900 (1997).
29. Pollard, D. & Thompson, S. L. Climate and ice-sheet mass balance at the last glacial maximum from the GENESIS version 2 global climate model. *Quat. Sci. Rev.* **16,** 841–864 (1997).
30. Pounds, J. A., Fogden, M. P. L. & Campbell, J. H. Biological response to climate change on a tropical mountain. *Nature* **398,** 611–615 (1999).

Acknowledgements. We thank J. A. Pounds for his Monteverde temperature and precipitation records and for sharing his observational data; J. A. Pounds, P. Colinvaux, H. Diaz, N. Graham, J. Harte, S. Hastenrath and J. Randerson for comments; D. Pollard for help with the GENESIS datasets (P.N.F.); T. Root for discussions (S.H.S.); and M. Schlesinger for the LCL data from the UI simulations. C.J.S. is supported by an EPA STAR graduate fellowship; S.H.S. acknowledges partial support from the Winslow Foundation.

Correspondence and requests for materials should be addressed to S.H.S. (e-mail: shs@leland.stanford.edu).

© 1999 Macmillan Magazines Ltd